

# Dynamic imaging of mitochondrial membrane proteins in specific sub-organelle membrane locations

Timo Appelhans<sup>1</sup> · Karin B. Busch<sup>1,2</sup> 

Received: 16 May 2017 / Accepted: 25 July 2017 / Published online: 17 August 2017

© International Union for Pure and Applied Biophysics (IUPAB) and Springer-Verlag GmbH Germany 2017

**Abstract** Mitochondria are cellular organelles with multifaceted tasks and thus composed of different sub-compartments. The inner mitochondrial membrane especially has a complex nano-architecture with cristae protruding into the matrix. Related to their function, the localization of mitochondrial membrane proteins is more or less restricted to specific sub-compartments. In contrast, it can be assumed that membrane proteins *per se* diffuse unimpeded through continuous membranes. Fluorescence recovery after photobleaching is a versatile technology used in mobility analyses to determine the mobile fraction of proteins, but it cannot provide data on sub-populations or on confined diffusion behavior. Fluorescence correlation spectroscopy is used to analyze single molecule diffusion, but no trajectory maps are obtained. Single particle tracking (SPT) technologies in live cells, such as tracking and localization microscopy (TALM), do provide nanotopic localization and mobility maps of mitochondrial proteins *in situ*. Molecules can be localized with a precision of between 10 and 20 nm, and single trajectories can be recorded and analyzed; this is sufficient to reveal significant differences in the spatio-temporal behavior of diverse mitochondrial proteins. Here, we compare diffusion coefficients obtained by these different technologies and discuss trajectory maps of diverse mitochondrial membrane proteins obtained by SPT/TALM. We show

that membrane proteins in the outer membrane generally display unhindered diffusion, while the mobility of inner membrane proteins is restricted by the inner membrane architecture, resulting in significantly lower diffusion coefficients. Moreover, tracking analysis could discern proteins in the inner boundary membrane from proteins preferentially diffusing in cristae membranes, two sub-compartments of the inner mitochondrial membrane. Thus, by evaluating trajectory maps it is possible to assign proteins to different sub-compartments of the same membrane.

**Keywords** Mitochondrial membrane proteins · TOM · TIM · hFis · Mitofilin/Mic60 · F<sub>1</sub>F<sub>0</sub> ATP synthase · Cox · Single molecule localization and diffusion · Mobility analyses · Membrane sub-compartments · SPT technologies · FRAP · FCS

Mitochondria are organelles with a plethora of functions, including Ca<sup>2+</sup> signaling, oxidation of fatty acids, respiration, ATP synthesis and recycling of redox-equivalents. To fulfill these tasks, mitochondria are subdivided into several compartments: the outer membrane (OM), the inner membrane (IM) and the matrix space. The IM is further compartmentalized into the inner boundary membrane (IBM) alongside the OM and the cristae membranes (CM) (Mannella et al. 2004) (Fig. 1). Despite the presence of 13 proteins that are mitochondrially encoded and part of the bioenergetic oxidative phosphorylation (OXPHOS) system, the complete repertoire of mitochondrial proteins (including further subunits of the OXPHOS) has to be imported via the translocase of the outer membrane (TOM) (Straub et al. 2016) and the translocase of the inner membrane (TIM) (Mokranjac and Neupert 2010). Furthermore, the complex IM architecture is under the control of several proteins, including F<sub>1</sub>F<sub>0</sub>ATP synthase (Gavin 2004; Paumard et al. 2002) and mitofilin/Mic60

This article is part of a Special Issue on ‘IUPAB Edinburgh Congress’ edited by Damien Hall

✉ Karin B. Busch  
buschkar@uni-muenster.de

<sup>1</sup> Mitochondrial Dynamics Group, School of Biology, University of Osnabrück, 49076 Osnabrück, Germany

<sup>2</sup> Institute of Molecular Cell Biology, School of Biology, Westfälische Wilhelms-University of Münster, 48149 Münster, Germany

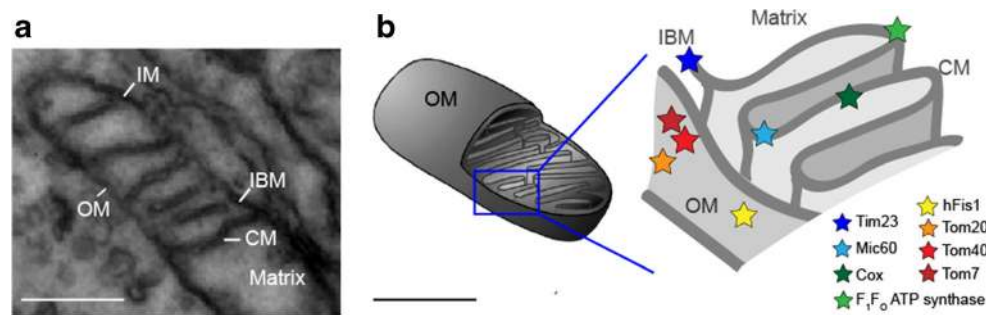


**Fig. 1** Ultrastructure of mitochondria and respective localization of important proteins. **a** Electron microscopy image showing part of a mitochondrion, with the membranes appearing black: OM outer membrane, IM inner membrane [which is partitioned into the inner boundary membrane (IBM) and the cristae membranes (CM)]. The matrix is an aqueous compartment. **b** Scheme showing the localization of the proteins that have been studied in terms of mobility and localization. *Tom40* Core subunit of the translocase of the outer

membrane (TOM) complex, *Tom20* receptor subunit of TOM, *Tom7* subunit of TOM (Shiota et al. 2015), *hFis1* human fission factor in the OM (Yu et al. 2005), *Mic60* mitofilin, part of the MICOS complex in the IBM (Ding et al. 2015), *Tim23* part of the inner membrane translocase (TIM) in the IBM (Demishtein-Zohary and Azem 2017), *Cox* cytochrome c oxidase, a complex of the oxidative phosphorylation (OXPHOS) system in the CM, *F<sub>1</sub>F<sub>0</sub>ATP synthase*, a further OXPHOS complex

(John 2005; Tarasenko et al. 2017). To better understand the function and interaction of these proteins, information on their specific sub-mitochondrial localization and spatio-temporal organization is needed (Fig. 1b). Superresolution fluorescence microscopy (including immuno-electron microscopy) has enabled sub-diffraction localization of mitochondrial molecules, resulting in the identification of proteins in different organelle compartments of mitochondria (Appelhans et al. 2012; Beinlich et al. 2015; Jans et al. 2013; Wurm and Jakobs 2006) and revealed that the proteins of the IM are apparently sub-compartmentalized in the IBM and CM part of the IM (Vogel et al. 2006). Information on the temporal dynamics of proteins would help to understand this segregation of proteins in an (in principle) continuous membrane. In the following, three dynamic methods to study mobility and to determine diffusion coefficients of mitochondrial membrane proteins are presented.

The mobility of several inner and outer membrane proteins (Sukhorukov et al. 2010) and of matrix–green fluorescent protein (Partikian et al. 1998) was determined by fluorescence recovery after photobleaching (FRAP), a method in which after spot bleaching the recovery of fluorescence is monitored and analyzed (Reits and Neefjes 2001) (Fig. 2a). The diffusion of a matrix-targeted protein was also determined via fluorescence correlation spectroscopy (FCS) (Koopman et al. 2007), which is not an imaging technology but a spectroscopic method that records changes in fluorescence intensity in the confocal volume over time (Bacia et al. 2006). From autocorrelation curves [ $G(\tau)$ ], the diffusion behavior is analyzed and diffusion coefficients are extracted (Fig. 2b).

Single particle tracking (SPT) combines the spatial and dynamic analysis of proteins by imaging single, labeled proteins at high frame rates until they are bleached. After localization, trajectory maps are generated by, for example, a multi-target tracing algorithm (Sergé et al. 2008) (Fig. 2c). Commonly, fluorescent protein-tags (FP) are used to visualize

the proteins of interest (Subach et al. 2010). In a variant of SPT, named tracking and localization microscopy (TALM) (Appelhans and Busch 2017; Appelhans et al. 2012), bright and photostable rhodamine dyes attached to a specific substrate reacting covalently with the HaloTag or SnapTag are used for post-translational labeling (Juillerat et al. 2003; Schröder et al. 2009). The localization and dynamics of several outer and inner membrane proteins have been analyzed using this method. From step length diagrams (Fig. 2c–II), apparent diffusion coefficients are extracted and appointed to subpopulations distinguished by their mobility (e.g. mobile, less mobile and confined mobile molecules). Mean square displacement plots of >30 ms allow for confinement analysis, following which only the diffusion coefficients of mobile fractions are compared.

### Movement of outer mitochondrial membrane proteins

The outer mitochondrial membrane is tubular without extra-investigations. To date, information on the mobility of four mitochondrial OM proteins is available: *hFis*, a protein involved in mitochondrial fission (Yu et al. 2005) and three different subunits of the TOM complex, i.e. *Tom7*, *Tom20* and *Tom40* (Shiota et al. 2015) (Fig. 1b). *hFis*, *Tom7* and *Tom20* possess a single transmembrane domain, while *Tom40* is a  $\beta$ -barrel protein inserted into the OM. The localization and mobility of *hFis* and *Tom7* were determined by FRAP analysis of FP-labeled proteins in mitochondria in situ in cell culture (Sukhorukov et al. 2010), and the obtained mobility was  $0.7 \mu\text{m}^2/\text{s}$  (*hFis*) and  $0.6 \mu\text{m}^2/\text{s}$  (*Tom7*), respectively (Table 1). The majority of *Tom7* molecules showed unhindered diffusion, but approximately 7% were immobile (Sukhorukov et al. 2010). In a different study, the mobility of *Tom40*, the core subunit of the TOM complex (Rapaport and Neupert 1999), was determined by SPT with a localization precision of

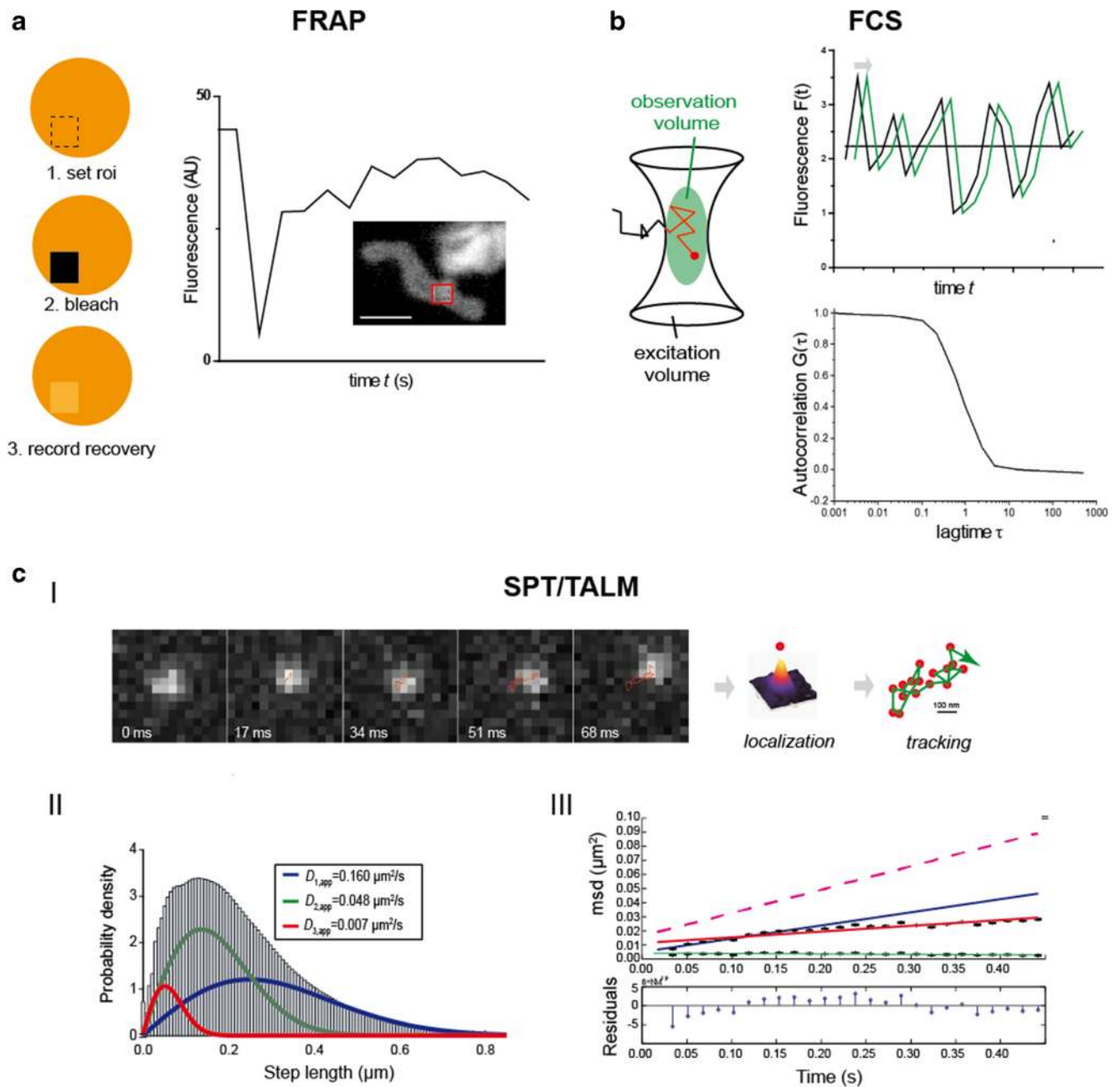


**Fig. 2** Technological methods to determine the mobility of mitochondrial proteins. **a** Fluorescence recovery after photobleaching (FRAP). Usually, proteins of interest are fused to a fluorescent protein and from a certain region of interest (roi) the pre-bleach fluorescence is recorded. Then, the fluorescence in the roi is bleached down and immediately after the recovery of fluorescence is monitored. The recovery curve is fitted and the percentage of mobile and immobile molecules and the diffusion coefficient of the mobile fraction can be determined. Here, a FRAP curve for Tom7, a subunit of the TOM complex, fused to green fluorescent protein is shown. The fluorescence was bleached in the indicated roi (red frame) (Sukhorukov et al. 2010). **b** Fluorescence correlation spectroscopy (FCS) reveals protein diffusion, such as in the mitochondrial matrix (Koopman et al. 2007). Fluorescence intensity fluctuations from the confocal volume are recorded and an autocorrelation function is generated from which the mean diffusion constant can be calculated. **c-I** Localization and tracking of single molecules in different

mitochondrial compartments by tracking and localization microscopy (TALM) (Appelhans et al. 2012), a single particle tracking (SPT) technique. A single molecule is observed for multiple frames until bleached. The fine localization of single molecules is obtained by two-dimensional Gaussian fitting of the diffracted signal in a deflection process, following which a trajectory map is generated using a multi-target tracing algorithm (Sergé et al. 2008). **c-II** Step length diagrams are generated, and from the cumulated distribution function (CDF) diffusion coefficients are extracted by fitting until the least root mean square error is minimized. Usually, several subpopulations characterized by different mobilities (mobile, less mobile and confined mobile) are obtained. **c-III** Mean square displacement (msd) plots are analyzed to obtain the confinement for short (2–5 steps, blue line) and long-range diffusion (2–20 steps, red line) (Schütz et al. 1997). The relation between msd and the diffusion coefficient  $D$  is:  $msd = 4D\Delta t^\alpha + 4\epsilon^2$  where  $\epsilon^2$  is the square error (localization precision) and  $\alpha$  is the non-linearity coefficient. Scale bar 100 nm (a)

**Table 1** Diffusion coefficients  $D$  of mitochondrial proteins in situ in live mammalian cells

Protein <sup>a</sup>	Mitochondrial localization	FRAP, $D$ ( $\mu\text{m}^2/\text{s}$ )	SPT/TALM, $D$ ( $\mu\text{m}^2/\text{s}$ )	FCS, $D$ ( $\mu\text{m}^2/\text{s}$ )
hFis	OM	$0.7 \pm 0.1$ Sukhorukov and Bereiter-Hahn (2009)	$0.170 \pm 0.05$ (90% mobile) Appelhans et al. (this paper)	
Tom7	OM	$0.6 \pm 0.4$ Sukhorukov and Bereiter-Hahn (2009)	$0.133 \pm 0.025$ Appelhans et al. (this paper)	
Tom20	OM		$0.142 \pm 0.014$ ; $0.005 \pm 5\text{E-}4$ Appelhans et al. 2012	
Tom40	OM		$0.5$ (% mobile) <sup>b</sup> (Kuzmenko et al. (2011))	
$\text{F}_1\text{F}_0$ ATP synthase, CV	IM	$0.4 \pm 0.1$ (mobile) $0.0005 \pm 0.0001$ (immobile) Sukhorukov and Bereiter-Hahn (2009)	$0.070 \pm 0.009$ (35%) (mobile) $0.020 \pm 0.004$ (47%) (less mobile) $0.005$ (18%) (immobile) Appelhans et al. (2012)	
Cox, CIV	IM	$0.3 \pm 0.07$ ; $0.007 \pm 0.002$ Sukhorukov and Bereiter-Hahn (2009)	$0.056 \pm 0.016$ (mobile) $0.016 \pm 0.005$ , less mobile $0.003 \pm 0.001$ , immobile Appelhans et al. (this paper)	
Mic60	IM		$0.068 \pm 0.001$ (49%) $0.020 \pm 0.004$ (51%) Appelhans et al. (this paper)	
Tim23	IM		$0.057 \pm 0.001$ (45%) Appelhans et al. (this paper)	
SDH	IM		$0.140 \pm 0.034$ (79%) $0.016$ (21%) Wilkins et al. (2012)	
Mt-FP	matrix	$22 \pm 2$ Partikian et al. (1998)		$20\text{--}30 \mu\text{m}^2/\text{s}$ Koopman et al. (2007)

FRAP Fluorescence recovery after photobleaching, FCS fluorescence correlation spectroscopy, SPT/TALM single particle tracking/tracking and localization microscopy, OM Outer membrane of mitochondrion, IM inner membrane of mitochondrion

<sup>a</sup> SDH Succinate dehydrogenase, Mt-FP mitochondrial fluorescence-labeled protein. All other proteins are defined in the caption of Fig. 1

<sup>b</sup> In isolated mitochondria from yeast

20 nm. Analysis of mean square displacements ( $msd$ ) within 5 ms and cumulative distribution functions (CDF) provided an apparent diffusion coefficient of  $D_{\text{app}} = 0.5 \mu\text{m}^2/\text{s}$  for Tom40, which is only marginal slower than the  $D$  for Tom7 obtained by

FRAP. For time windows above 35 ms, the diffusion was clearly confined. Several reasons were discussed for the confinement: a complicated geometry, interaction with lipids or an active, anchored complex (Kuzmenko et al. 2011). In

complementary studies, hFis and Tom20 mobilities were determined by TALM, a specific SPT method (Appelhans and Busch 2017; Appelhans et al. 2012). Apparent diffusion coefficients were  $D_{\text{mobile, hFis}} = 0.17 \mu\text{m}^2/\text{s}$  for hFis and  $D_{\text{mobile, Tom20}} = 0.142 \mu\text{m}^2/\text{s}$ . The obtained trajectory maps of hFis1 and Tom20 show rather unhindered diffusion for the majority of proteins (Fig. 3a-I, 3a-II) with a random directionality. The calculated localization precision was 10 nm on average, although a subpopulation of 14% of hFis and Tom20 had a diffusion coefficient of  $D < 0.009 \mu\text{m}^2/\text{s}$ , indicating immobile/confined fractions (as also found for Tom7 in FRAP measurements). Alternatively, this can be an outcome of movement in  $z$ . Movement in  $z$  gives small step lengths in two-dimensional (2D) projections and thus results in low diffusion coefficients. A correction taking into account the geometry resulted in an increase in the diffusion coefficients to  $D_{\text{app,corr}} = 0.215 \mu\text{m}^2/\text{s}$  for Tom20 and  $D_{\text{app,corr}} = 0.410 \mu\text{m}^2/\text{s}$  for hFis (Appelhans et al. 2012), which are still lower than those obtained from FRAP studies ( $D=0.6$  and  $D=0.7 \mu\text{m}^2/\text{s}$ , respectively).

### Movement of inner mitochondrial membrane proteins

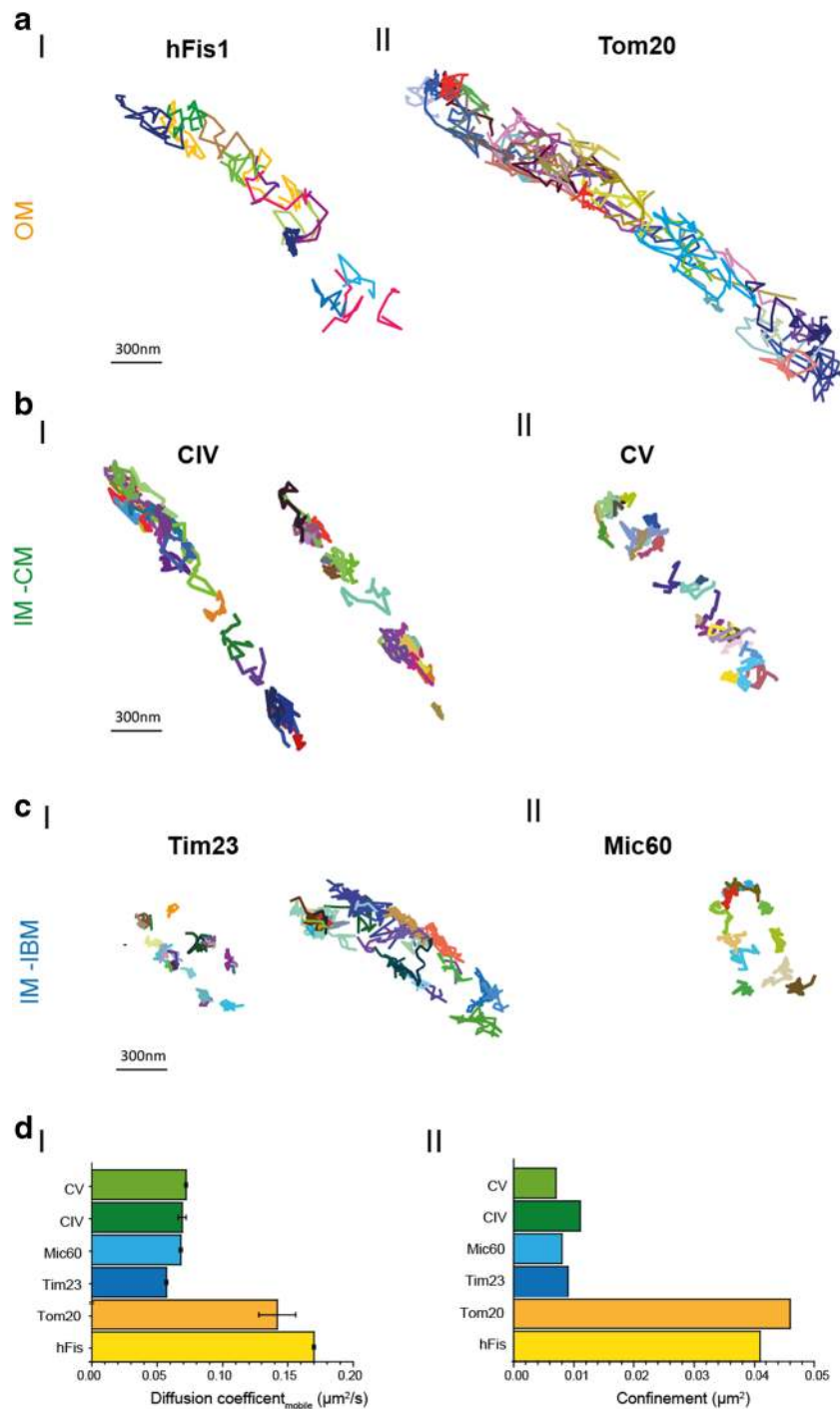
The mobility of inner mitochondrial membrane proteins Cox and  $F_1F_0$  ATP synthase, both complexes of the oxidative phosphorylation system (CIV and CV of OXPHOS), was determined by FRAP (Sukhorukov et al. 2010) and yielded diffusion coefficients of  $D = 0.3 \mu\text{m}^2/\text{s}$  (Cox) and  $D = 0.4 \mu\text{m}^2/\text{s}$  ( $F_1F_0$  ATP synthase). In a complementary study, diffusion analysis by TALM resulted in  $D_{\text{app,Cox}} = 0.056 \mu\text{m}^2/\text{s}$  and  $D_{\text{app, } F_1F_0 \text{ ATP synthase}} = 0.070 \mu\text{m}^2/\text{s}$  (Table 1). TALM trajectory maps also show details about possible confinement and directionality. Contrary to OM proteins (Fig. 3a), the trajectory maps of Cox and  $F_1F_0$  ATP synthase indicate a confinement of those specific IM proteins in cristae (Fig. 3b). In contrast, trajectory maps of the IM proteins Tim23 and Mic60 show a different type of confinement: the trajectories are found in a pearl-like arrangement along both sides of the IBM with no preferential directionality (Fig. 3c). The diffusion coefficient for Tim23 was  $D_{\text{mobile, Tim23}} = 0.044 \mu\text{m}^2/\text{s}$  ( $\pm 0.025 \mu\text{m}^2/\text{s}$ ;  $N = 2$  independent assays, >1900 trajectories analyzed); for Mic60 it was  $D_{\text{mobile, Mic60}} = 0.063 \mu\text{m}^2/\text{s}$  ( $\pm 0.010 \mu\text{m}^2/\text{s}$ ;  $N = 2$  independent assays, >2000 trajectories analyzed). Albeit the diffusion coefficients of both proteins were similar to those of Cox and  $F_1F_0$  ATP synthase in the same membrane, their specific localization was clearly distinct as the trajectory maps revealed (Fig. 3c).

The apparent diffusion coefficients for the IM proteins Cox and  $F_1F_0$  ATP synthase determined by TALM were significantly lower than those obtained by FRAP, likely due to a significant quota of molecules being restricted in their diffusion due to geometrical constraints. When *msd* were plotted,

for long range diffusion >50 ms, confinement started to dominate the mobility in accordance with preferential localization in cristae membranes (Wilkins et al. 2012) (Fig. 3d-II). These confined mobile molecules were probably not recorded by FRAP, since their confinement within  $0.01 \mu\text{m}^2$  (Fig. 3c-II) is below the diffraction limit. For Tim23 and Mic60, the confinement was in a similar range, albeit for a different reason: these molecules are anchored in the membrane in conjunction with supercomplex formation (Harner et al. 2011; van der Laan et al. 2016).

### Conclusion

The determination of protein mobility in mitochondrial compartments is still a challenge. FCS, which is an established method for the determination of the mobility of soluble proteins, has had no application in the determination of mitochondrial membrane protein mobility, but only for a matrix-targeted soluble FP. The determined diffusion coefficient was similar to that determined by FRAP (Table 1). Indeed, FCS and FRAP are probably the only methods to characterize the mobility of matrix proteins, since diffusion coefficients attributed to soluble FPs are  $>93 \mu\text{m}^2/\text{s}$  (Petrasek and Schwill 2008) and the corresponding step lengths are too large to obtain confident connections between subsequent localizations in SPT. The reduced mobility of FPs with  $20\text{--}30 \mu\text{m}^2/\text{s}$  in the mitochondrial matrix is probably related to diffusion obstacles imposed by cristae membranes dividing the matrix (Sukhorukov and Bereiter-Hahn 2009). For membrane proteins, FRAP studies have provided higher diffusion coefficients as SPT analysis, possibly attributable to two factors: (1) FRAP is a diffraction-limited imaging technique and thus is spatially coarse; (2) FRAP measures only highly mobile molecules, since confined molecules or slow mobile molecules are too slow to contribute to a fluorescence recovery. In addition, the bleaching which continues during recording is more of a problem for FRAP than for single molecule imaging (whereby the signal is lost, but has no influence on the analysis). Furthermore, recovery analysis after spot photobleaching of FP in mitochondria is not straightforward to analyze due to geometrical factors, shape changes and the movement of mitochondria themselves (Dikov and Bereiter-Hahn 2013; Mishra and Chan 2016). This also partially impacts SPT analysis and a thorough review of data is necessary. Mitochondrial movement interfering with protein motility can be revealed by superimposing images of mitochondria taken before and after the FRAP analysis or superimposing the first and last 500 frames of SP imaging. The power of single molecule tracking in contrast to FRAP and FCS is that it provides localization and trajectory maps and thus enables sub-organellar resolution. Based on the pattern of their trajectory maps, Tim23 and Mic60 could be designated to the IBM in line with a functional localization at interaction sites with the TOM complex (Tim23) and the cristae junctions (Mic60)



(van der Laan et al. 2016), while Cox (CIV) and  $F_1F_0$  ATP synthase (CV) could be appointed to cristae membranes, which are the site of OXPHOS. On the other hand, in SPT/TALM, the diffusion coefficients are extracted from 2D projected movement, which results in an underestimation of mobility on tubular or spherical structures (Renner et al. 2011). Albeit a variety of methods for obtaining both 3D super-resolution images and 3D tracking information have been devised (von Diezmann et al. 2017), 3D tracking is still a challenging option and to our

knowledge has not yet been applied to the analysis of the mobility of mitochondrial proteins. Hitherto, even 2D SPT/TALM has been feasible to elucidate sub-organelle localization from the pattern of the respective trajectory maps. To summarize, FRAP and SPT/TALM are complementary methods revealing different aspects of the spatio-temporal organization of proteins.

**Acknowledgments** The authors would like to thank Wladislaw Kohl for technical advice and support. We also wish to express our gratitude to

◀ **Fig. 3** Motility analysis of mitochondrial membrane proteins by SPT/TALM. **a** Trajectory maps of OM proteins hFis (**a-I**) and Tom20 (**a-II**). **b-I** Trajectory maps of Tim32 preferentially found in the IBM. **b-II** Map of Mic60, which is part of the MICOS complex, at cristae junctions (Zerbes et al. 2012). **c-I** Trajectory maps of Cox labeled at its subunit CoxVIIIa in two mitochondria. **c-II** Trajectory map of  $F_1F_0$  ATP synthase labeled at subunit  $\gamma$ . For fluorescence labeling of these different protein species, C-terminal HaloTag®-fusion (Los et al. 2008) proteins were generated and posttranslationally labeled by membrane-permeable tetramethylrhodamine functionalized with the HaloTag®-Ligand (TMR<sup>HTL</sup>). TMR<sup>HTL</sup> in the specific mitochondrial environment turned out to be a photostable and bright emitter (Appelhans et al. 2012). The labeling was done with substoichiometric concentrations of TMR<sup>HTL</sup> (0.5–1 nM) to obtain single molecule signals that can be distinguished and localized. The dye was excited with a diode pumped solid-state laser (excitation 561 nm, 200 mW; Cobolt Jive 561 nm, Cobolt), and single molecule signals were recorded with a back-illuminated electron multiplying charged coupled device EMCCD camera (model iXON 897, pixel size 16  $\mu\text{m}^2$ ; Andor Technology Ltd., Belfast, UK). The mitochondrial localization of the constructs was tested by co-staining with MitoTracker®DeepRed (not shown). The signal of a single particle was recorded over time until bleaching and analysed by the multi-target tracer algorithm (Sergé et al. 2008), generating a trajectory of the respective molecule. The magnification is the same for all trajectory maps. **d-I** Apparent diffusion coefficients  $D_{\text{app}}$  for mobile fraction of OM and IM proteins. **d-II** Confinement for OM and IM proteins

Christian Richter for evaluation software. The study was supported by the CRC SFB944 and CiM/Münster.

**Author contributions** Conception and design: K.B., T.A. Acquisition of data: T.A.; K.B. Analysis and interpretation of data: T.A., K.B. Drafting or revising the article: K.B.

#### Compliance with ethical standards

**Conflict of interest** Timo Appelhans declares that he has no conflicts of interest. Karin B. Busch declares that she has no conflicts of interest.

**Ethical approval** This article does not contain any studies with human participants or animals performed by any of the authors.

## References

- Appelhans T, Busch K (2017) Single molecule tracking and localization of mitochondrial protein complexes in live cells. *Methods Mol Biol* 1567:273–291. doi:10.1007/978-1-4939-6824-4\_17
- Appelhans T, Richter C, Wilkens V et al (2012) Nanoscale organization of mitochondrial microcompartments revealed by combining tracking and localization microscopy. *Nano Lett* 12:610–616. doi:10.1021/nl203343a
- Bacia K, Kim SA, Schwille P (2006) Fluorescence cross-correlation spectroscopy in living cells. *Nat Methods* 3:83–89. doi:10.1038/nmeth822
- Beinlich F, Drees C, Piehler J, Busch K (2015) Shuttling of PINK1 between mitochondrial microcompartments resolved by triple-color Superresolution microscopy. *ACS Chem Biol* 10:1970–1976. doi:10.1021/acscchembio.5b00295
- Demishtein-Zohary K, Azem A (2017) The TIM23 mitochondrial protein import complex: function and dysfunction. *Cell Tissue Res* 367:33–41. doi:10.1007/s00441-016-2486-7

- Dikov D, Bereiter-Hahn J (2013) Inner membrane dynamics in mitochondria. *J Struct Biol* 183:455–466. doi:10.1016/j.jsb.2013.06.003
- Ding C, Wu Z, Huang L et al (2015) Mitofilin and CHCHD6 physically interact with Sam50 to sustain cristae structure. *Sci Rep* 5:16064. doi:10.1038/srep16064
- Gavin PD (2004) Cross-linking ATP synthase complexes in vivo eliminates mitochondrial cristae. *J Cell Sci* 117(11):2333–2343
- Harner M, Neupert W, Deponte M (2011) Lateral release of proteins from the TOM complex into the outer membrane of mitochondria. *EMBO J* 30:3232–3241. doi:10.1038/emboj.2011.235
- Jans DC, Wurm CA, Riedel D et al (2013) STED super-resolution microscopy reveals an array of MINOS clusters along human mitochondria. *Proc Natl Acad Sci USA* 110:8936–8941. doi:10.1073/pnas.1301820110
- John GB (2005) The Mitochondrial Inner Membrane Protein Mitofilin Controls Cristae Morphology. *Mol Biol Cell* 16(3):1543–1554
- Juillerat A, Gronemeyer T, Keppler A et al (2003) Directed evolution of O6-Alkylguanine-DNA alkyltransferase for efficient labeling of fusion proteins with small molecules in vivo. *Chem Biol* 10:313–317. doi:10.1016/s1074-5521(03)00068-1
- Koopman W, Hink M, Verkaar S et al (2007) Partial complex I inhibition decreases mitochondrial motility and increases matrix protein diffusion as revealed by fluorescence correlation spectroscopy. *Biochim Biophys Acta* 1767:940–947. doi:10.1016/j.bbabi.2007.03.013
- Kuzmenko A, Tankov S, English BP et al (2011) Single molecule tracking fluorescence microscopy in mitochondria reveals highly dynamic but confined movement of Tom40. *Sci Rep* 1:195. doi:10.1038/srep00195
- Los G, Encell L, McDougall M et al (2008) HaloTag: a novel protein labeling technology for cell imaging and protein analysis. *ACS Chem Biol* 3:373–382. doi:10.1021/cb800025k
- Mannella C, Marko M, Penczek P et al (2004) The internal compartmentation of rat-liver mitochondria: tomographic study using the high-voltage transmission electron microscope. *Microsc Res Tech* 27:278–283. doi:10.1002/jemt.1070270403
- Mishra P, Chan D (2016) Metabolic regulation of mitochondrial dynamics. *J Cell Biol* 212:379–387. doi:10.1083/jcb.201511036
- Mokranjac D, Neupert W (2010) The many faces of the mitochondrial TIM23 complex. *Biochim Biophys Acta* 1797:1045–1054. doi:10.1016/j.bbabi.2010.01.026
- Partikian A, Olveczky B, Swaminathan R et al (1998) Rapid diffusion of green fluorescent protein in the mitochondrial matrix. *J Cell Biol* 140:821–829. doi:10.1083/jcb.140.4.821
- Paumard P, Vaillier J, Couly B, Schaeffer J, Soubannier V, Mueller DM, Brèthes D, di Rago J-P, Velours J (2002) The ATP synthase is involved in generating mitochondrial cristae morphology. *EMBO J* 21(3):221–230
- Petrasek Z, Schwille P (2008) Precise measurement of diffusion coefficients using scanning fluorescence correlation spectroscopy. *Biophys J* 94:1437–1448. doi:10.1529/biophysj.107.108811
- Rapaport D, Neupert W (1999) Biogenesis of Tom40, core component of the tom complex of mitochondria. *J Cell Biol* 146:321–332. doi:10.1083/jcb.146.2.321
- Reits E, Neeffjes J (2001) From fixed to FRAP: measuring protein mobility and activity in living cells. *Nat Cell Biol* 3:E145–E147. doi:10.1038/35078615
- Renner M, Domanov Y, Sandrin F et al (2011) Lateral diffusion on tubular membranes: quantification of measurements bias. *PLoS One* 6:e25731. doi:10.1371/journal.pone.0025731
- Schröder J, Benink H, Dyba M, Los G (2009) In vivo labeling method using a genetic construct for nanoscale resolution microscopy. *Biophys J* 96:L1–L3. doi:10.1016/j.bpj.2008.09.032
- Schütz GJ, Schindler H, Schmidt T (1997) Single-molecule microscopy on model membranes reveals anomalous diffusion. *Biophys J* 73(2):1073–1080

- Sergé A, Bertaux N, Rigneault H, Marguet D (2008) Dynamic multiple-target tracing to probe spatiotemporal cartography of cell membranes. *Nat Methods* 5:687–694. doi:10.1038/nmeth.1233
- Shiota T, Imai K, Qiu J et al (2015) Molecular architecture of the active mitochondrial protein gate. *Science* 349:1544–1548. doi:10.1126/science.aac6428
- Straub SP, Stiller SB, Wiedemann N, Pfanner N (2016) Dynamic organization of the mitochondrial protein import machinery. *Biol Chem* 397:1097–1114. doi:10.1515/hsz-2016-0145
- Subach FV, Patterson GH, Renz M et al (2010) Bright monomeric photoactivatable red fluorescent protein for two-color super-resolution sptPALM of live cells. *J Am Chem Soc* 132:6481–6491. doi:10.1021/ja100906g
- Sukhorukov V, Bereiter-Hahn J (2009) Anomalous diffusion induced by cristae geometry in the inner mitochondrial membrane. *PLoS One* 4:e4604. doi:10.1371/journal.pone.0004604
- Sukhorukov VM, Dikov D, Busch K et al (2010) Determination of protein mobility in mitochondrial membranes of living cells. *Biochim Biophys Acta* 1798:2022–2032. doi:10.1016/j.bbame.2010.07.016
- Tarasenko D, Barbot M, Jans DC et al (2017) The MICOS component Mic60 displays a conserved membrane-bending activity that is necessary for normal cristae morphology. *J Cell Biol* 216:889–899. doi:10.1083/jcb.201609046
- van der Laan M, Horvath SE, Pfanner N (2016) Mitochondrial contact site and cristae organizing system. *Curr Opin Cell Biol* 41:33–42. doi:10.1016/j.ceb.2016.03.013
- Vogel F, Bornhövd C, Neupert W, Reichert A (2006) Dynamic subcompartmentalization of the mitochondrial inner membrane. *J Cell Biol* 175:237–247. doi:10.1083/jcb.200605138
- von Diezmann A, Shechtman Y, Moerner WE (2017) Three-dimensional localization of single molecules for super-resolution imaging and single-particle tracking. *Chem Rev* 117:7244–7275. doi:10.1021/acs.chemrev.6b00629
- Wilkens V, Kohl W, Busch K (2012) Restricted diffusion of OXPHOS complexes in dynamic mitochondria delays their exchange between cristae and engenders a transitory mosaic distribution. *J Cell Sci* 126:103–116. doi:10.1242/jcs.108852
- Wurm C, Jakobs S (2006) Differential protein distributions define two sub-compartments of the mitochondrial inner membrane in yeast. *FEBS Lett* 580:5628–5634. doi:10.1016/j.febslet.2006.09.012
- Yu T, Fox RJ, Burwell LS, Yoon Y (2005) Regulation of mitochondrial fission and apoptosis by the mitochondrial outer membrane protein hFis1. *J Cell Sci* 118:4141–4151. doi:10.1242/jcs.02537
- Zerbes R, Bohnert M, Stroud D et al (2012) Role of MINOS in mitochondrial membrane architecture: cristae morphology and outer membrane interactions differentially depend on mitofilin domains. *J Mol Biol* 422:183–191. doi:10.1016/j.jmb.2012.05.004